Hydrology and Earth System Sciences, 4(1), *141–153* (2000) © EGS

Hydrology & Earth System Sciences

The role of olive trees in rainfall erosivity and runoff and sediment yield in the soil beneath

E. de Luna[1], A. Laguna[2] and J.V. Giráldez[3]

[1]Department of Soils and Irrigation, CIFA. Apdo. 3092, 14080 Córdoba, Spain
[2]Department of Applied Physics, University of Córdoba, Apdo. 3048, 14080 Córdoba, Spain
[3]Department of Agronomy, University of Córdoba, Apdo 3048, 14080 Córdoba, Spain
e-mail for corresponding author: aglgicej@uco.es

Abstract

The modification of raindrops by the canopy of olive trees increases the kinetic energy of the rain per unit area. The kinetic energy computed from the measured drop size distribution under the tree canopy in simulated rainfall experiments is greater than that received in the open, 17.1 J mm^{-1}, as against 15.7 J mm^{-1}. This causes higher soil detachment and loss than that observed outside the canopy. Tillage treatments of the soil modify its erodibility, accelerate soil detachment and reduce, simultaneously, the velocity of runoff. Both effects reduce the amount of sediment compared to that observed in the non-tilled soil. The average values of soil lost per unit of rain depth and unit area were 5.81 g $mm^{-1}m^{-2}$ (conventional tillage) and 4.02 g $mm^{-1}m^{-2}$ (zero tillage) under the canopy compared to 0.89 g mm^{-1} m^{-2} (conventional tillage) and 0.95 g mm^{-1} m^{-2} (zero tillage) in the open.

Introduction

Traditionally, vegetative cover has been accepted as a good soil conservation practice. The canopy above and the litter at ground level protect the soil from the impact of raindrops, reduce the velocity and energy of surface runoff and, by reducing the loss of water by evaporation, maintain the resistance of soil aggregates against erosive agents. However, when soil cover is not complete, or if the canopy is too high above the ground, the protective function may be far from perfect, and even negative, so that the aggressive effects of the rain are increased.

Olive tree cropping is a traditional agricultural system in Mediterranean countries because olives by their ability to endure long hot and dry periods, are so well adapted to the extremes of the Mediterranean climate. The competition for water between the olives and weeds forces the farmer to control the latter, usually by intensive tillage. In the past, olive cropping was confined mainly to hilly lands, because of its susceptibility to root infections under waterlogged conditions and to the dedication of lowlands to more profitable crops such as cereals or irrigated crops. The combination of reduced cover, frequent tillage and steep lands induced great soil losses by erosion. New techniques to control soil erosion, such as zero tillage or chemical weed control, were introduced successfully in Spain by Pastor (1987) in the seventies. The reduced root damage, caused by excessive disk harrowing in the past, and the lower incidence of killer frost in winter, attributed to the greater radiative transfer of energy from the flatter soil surface to the tree leaves during the winter, resulted in a net increase in yield when compared to traditional tillage systems. At the same time, soils under zero tillage develop a surface crust, which, while protecting the soil against raindrop impact or the shearing effects of surface runoff, reduces water infiltration rates (Giráldez *et al.*, 1990).

The higher runoff yield of zero tilled soils led to higher erosion losses than those observed in conventionally tilled soils. Nowadays, new systems of cover crops are being tested to reduce soil losses. Despite the importance of the olive tree for the agriculture and economy of the Mediterranean countries, not much information on soil erosion is available.

Tree canopies may act as rainwater collectors, or *reverse umbrellas*, as stated by Clothier (1978), quoted by Zhai *et al.* (1990). The canopy catches the raindrops falling in any direction and part is conveyed through branches and trunk to the root zone. Raindrops reduced to droplets return to the atmosphere by evaporation or run down along branches and trunk to the ground, or coalesce into larger drops. Several parameters have been proposed to assess the erosive action of the rain. Kinetic energy is a reasonably good index of soil detachment (e.g. Sharma *et al.*, 1993). The Universal Soil Loss Equation bases its erosivity factor partly on the kinetic energy of the rain. However, other authors such as Rose (1960) have found a better correlation of soil

detachment by raindrops with the momentum than with the kinetic energy of the rain. Force is a consequence of the momentum change, and may be more related to the breakdown of aggregates than the kinetic energy. Other factors, especially the soil characteristics, are involved in the rupture of soil aggregates (Nearing, 1987). The impact of water drops generates pressure waves, which stress the soil skeleton and soil pores. The boundary shear stress of the water drop impact depends on drop mass and terminal velocity (Hartley and Alonso, 1991).

The size distribution of raindrops has been analyzed in many fields, such as meteorology. Many of the proposed equations are represented in a general formula by Sempere-Torres *et al.* (1994).

The number of drops whose diameter lie in the (D, $D + dD$) range, per unit air volume, N, may be expressed as,

$$N(D,\psi) = \psi^a f(D\psi^{-b}) \qquad (1)$$

where ψ is a reference variable and a and b are two parameters. The widely used Marshall and Palmer equation (Rogers and Yau, 1991, chap. 10, eq. 10.1), is derived from (1) where $\psi = r$ is the rainfall rate, $a = 0$ and $b = 0.21$, and $f()$ represents the exponential function. This distribution is modified by the canopy interception.

This report presents the results of a study of the water erosion process in Southern Spain in olive cropped soils tilled both traditionally and chemically.

Material and methods

The experiments were carried out in the Alameda del Obispo Experimental Station near Córdoba, in Southern Spain. The soils of the farm are very fine, montmorillonitic, thermic, typic xerofluvent and are on a gentle uniform slope of 15%. Two small plots with one olive tree at the centre were chosen, one under conventional tillage 24.35 m^2 in size, and the other with chemical weed control 28.65 m^2 in size. Both plots were delimited with metal sheets to prevent runoff from outside. Another metal boundary was set up within each plot to separate the volume of runoff produced by the rain falling from the canopy (Fig. 1a and b). The canopy projected area is 4.68 m^2 in the conventional tillage plot and 7.48 m^2 in the zero tillage plot.

A rainfall simulator was developed with four sectoral sprinklers (VYR 20) located at the corners of the plots on 5 m high poles, connected by pipes in a closed circuit arrangement. Before the experiments, the rainfall uniformity was measured in a plot without an olive tree by two networks each of 36 rain gauges, one disposed regularly on a plane 2.9 m high over the mean level to avoid canopy effects, and another one with the gauges on the ground surface. Rainfall distribution from one of them is presented in Fig. 2. As the trials were carried out in the open, the wind was a very important factor, as it moved the rain mass from one

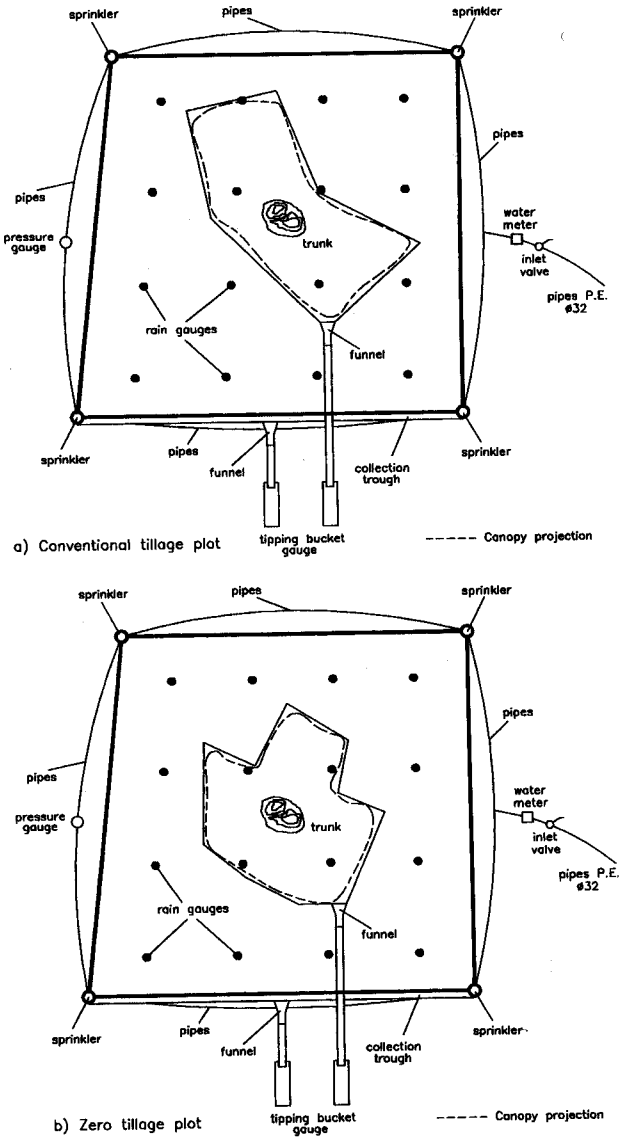

Fig. 1. *Experimental set up.*

direction to another. There was a higher rainfall concentration in the centre of the plot due to the disposition of the sprinklers. The differences were much less at ground level. The uniformity coefficient for rainfall distribution on the ground surface without an olive tree was 0.64; on a plane 2.9 m above the ground, it was 0.61. During the rainfall simulation runs, the total rainfall amount and distribution were measured by 16 rain gauges disposed regularly on the ground surface. Runoff water was measured at the two outlets with tipping bucket gauges similar to those used by Barfield and Hirschi (1986), with an automatic data recorder. Water was sampled during every rainfall trial to measure the concentration of solids. A granulometric analysis was made on the solid residue, using the hydrometer method according to Gee and Bauder (1986). The stemflow was separated in some trials by the standard

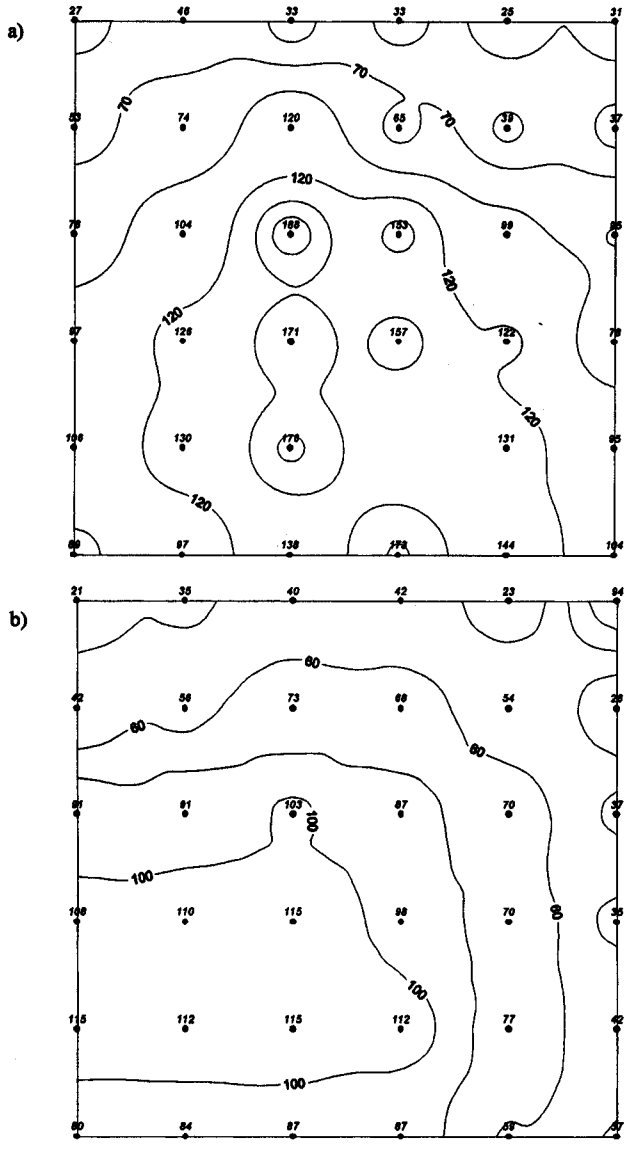

Fig. 2. *Spatial distribution of simulated rainfall depth (mmh^{-1}) in a 5 × 5 m^2 plot without an olive tree: (a) at a height of 2.9 m and (b) at ground level. Black points indicate the position of rain gauges with their respective recorded rainfall depth (mmh^{-1}). Contour lines are computed using the reciprocal of the square of the distance as interpolation method. Duration of rain: 30 min. Nozzle pressure: 221 kPa.*

method of fitted rubber collars around the trunk to trap water flowing down. During the simulation runs, wind speed and direction, temperature, and relative humidity of the air were measured with a standard automatic weather station. Soil moisture was sampled at 5 points randomly chosen in the plot, before and after every trial (Gardner, 1986).

Drop size distribution was determined by the method developed by Eigel and Moore (1983). Raindrops were collected in a Petri dish (diameter: 9.5 cm; depth: 1.4 cm) containing SAE 90 oil. Drops of diameter greater than 1.65 mm were deformed in the time interval between drop capture and the photograph. The method was calibrated with water drops of known volume made with a micropipette, to determine the diameter, D_o, equivalent to the diameter of the undeformed drop. The total number of drops used was 88, with 11 different diameters between 1.35 and 8.5 mm and 8 repetitions for each size. The equation relating the diameter of spherical drops to the deformed section in the oil layer was

$$D_o = 0.18 + 0.89D \quad (2)$$

where D is the diameter measured in oil, in mm, and the correlation coefficient was 0.95885.

The photograph was made with dark-field illumination, where all the incoming light passes through the Petri dish. Drop diameters were recorded using an image analyser, consisting of a digitizer card DT-2851 with 512 × 512 pixels, and 256 grey levels, a solid state chamber, and a source code, IMAGO, created by the University of Córdoba Image Analysis Service.

Drop size distribution changes under the canopy of the olive tree

Raindrops coalesce in their fall through the atmosphere and form drops of larger diameter, which may deform and even break down before they reach any surface. The largest size of water drops not breaking down in experiments in wind tunnels and air columns under low turbulence, was 4.5 mm (Pruppacher and Klett, 1980). Gunn and Kinzer (quoted by Park *et al.*, 1983), found an upper instability diameter of 6 mm, but Beard (1976) recorded 7 mm raindrops.

The reference variable in Eqn. (1) is related to rainfall rate. One parameter of the drop size distribution, the median volume drop diameter, D_{50}, may be written as a function of the rainfall rate using a power expression (Laws and Parson, 1943). Sempere-Torres *et al.* (1992) accepted as a good estimate for their Mediterranean rainfall data:

$$D_{50} = 1.24r^{.182} \quad (3)$$

Rainfall rate is in mm h^{-1}, and drop diameter in mm. For the average rainfall rate of the simulator described, a value of D_{50} = 2.4 mm was found. This value is higher than the value derived from the drop size distribution of the simulator, D_{50} = 1.5 mm, represented in Fig. 3. Simulated rain is finer and, consequently, less erosive than natural rain with otherwise equivalent characteristics.

Raindrop size distribution under and outside the canopy (Fig. 3) shows the enlargement due to the interception process. The numbers of drops randomly collected under the canopy and from the simulator were 845 and 384 respectively. According to the results of Salles *et al.* (1999), these numbers of drops may lead to an uncertainty of at least

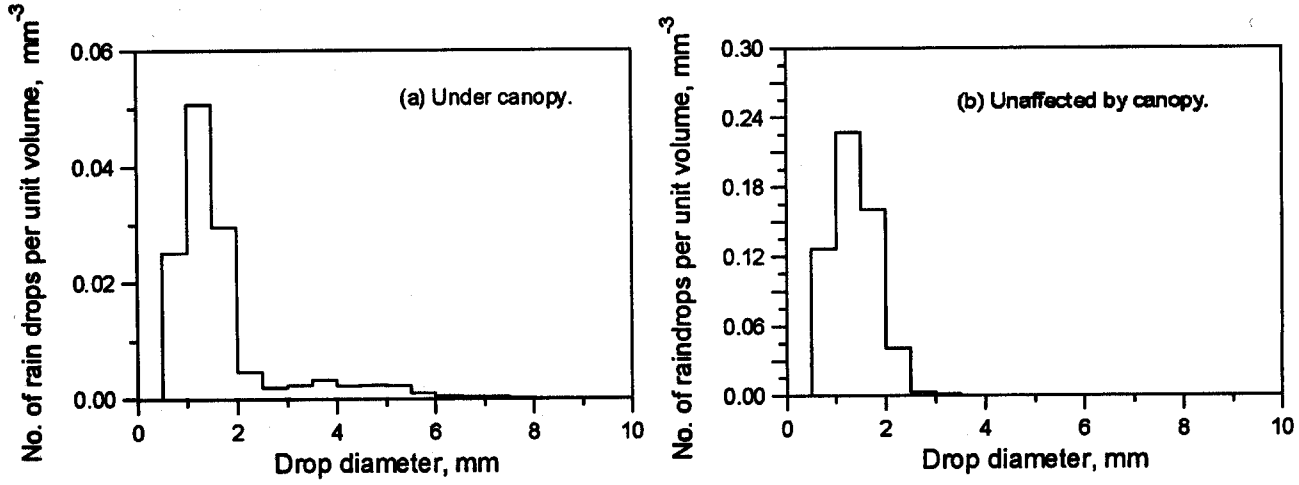

Fig. 3. *Drop size distribution, obtained with simulated rainfall, expressed as number of rain drops in each size range, per unit water volume. a) Under canopy. b) Unaffected by canopy.*

7 to 10 per cent in the estimation of the global parameters such as D_{50} and kinetic energy. To determine the drop size distribution, 10 Petri dish collectors were analysed for drops from under the tree and 3 for drops from the simulator. The olives, branches, and leaves of the tree gave rise to different sizes of drop, so that the number of Petri dishes analysed was higher under the canopy than outside. The drops collected outside the canopy lay in the 0.5–3 mm diameter range. Drops falling from the canopy are up to 8 mm in diameter.

The modification of the original distribution was found to be dependent on the stage of development of the vegetation. Different plant elements in the coalescence process contribute to a wide range of drop diameters. The largest drops fall from the olive fruits, intermediate drops come from the leaves, whereas the smallest ones are splashed or belong to the simulated rainfall out of the canopy.

Raindrop size distributions are represented in Fig. 3. They can be split into two different distributions of canopy drop size (Brandt, 1989). One is similar to the distribution of rain in the open, with an apparent upper value of 2.5 mm, which can be attributed to the throughfall population. The other ranges in diameter from 2.5 to 8 mm and results from the water dripping from the canopy. The residual population, after subtraction of the throughfall drops, is independent of both rainfall rate and canopy characteristics and can be approximated by a Gaussian distribution with a mean value close to 5 mm. For drops greater than 2.5 mm in diameter, the mean diameter was 4.3 mm in the present study.

Assouline and Mualem (1989) suggested one version of that function,

$$F(D,r) = 1 - \exp(-\alpha D^{\beta}) \qquad (4)$$

where $F(D, r)$ is the fraction of liquid water in the unit volume of air consisting of drops with diameters in the range $(D, D + dD)$, and α and β are two parameters. Normalizing diameters, $D^* = D/\overline{D}$. With $\overline{D}$ as a reference diameter, Eqn. (4) becomes:

$$F(D^*,r) = 1 - \exp(-\gamma D^{*\beta}) \qquad (5)$$

The parameters of the Weibull fit are shown in Table 1. These values are not far from those obtained by Assouline and Mualem (1989) and are almost universal and independent of place and rainfall type.

Impact velocity of water drops on the soil surface

When a water drop falls through the atmosphere, its

Table 1. Parameters of the Weibull fit to drop size distribution under and outside the canopy of olive trees, compared to those found by Assouline and Mualem, (1989). The correlation coefficients correspond to the double logarithmic transformation that leads to a linear relationship.

	Simulated rainfall	Under the canopy	Assouline and Mualem (1989)
β	2.95	2.34	3.00
γ	0.73	0.73	0.71
corr. coef.	0.98	0.99	

movement is determined by gravity and buoyancy effects, F_g,

$$F_g, = (\rho_w - \rho_a)Vg \quad (6)$$

where ρ_w and ρ_a are the densities of liquid water and air, respectively, V is the drop volume, g the acceleration due to gravity, and F_r is friction

$$F_r = 1/2 C_d \rho_a A v^2 \quad (7)$$

where C_d is the drag coefficient, A the projected surface of the drop in the direction of fall and v the velocity. This movement is accelerated at a rate decreasing with time until it reaches zero. Thereafter, the forces of gravity and of buoyancy effects become equal and the velocity assumes a constant value, the terminal velocity, v_t.

Introducing the Reynolds number, $R_e = v_t D/\nu$, where ν is the kinematic viscosity of the air, the terminal velocity is

$$v_t = \frac{4}{3}\frac{p_w - p_a}{p_a}\frac{D^2 g}{C_d R_e \nu} \approx \frac{4}{3}\frac{g p_w D^2}{\mu C_d R_e} \quad (8)$$

with μ as the dynamic viscosity of the air, neglecting air density with respect to liquid water density. For low values of the Reynolds number, $C_d R_e/24$ approaches unity, yielding a quadratic dependence of v_t on the diameter. This and other simplifications allow an approximation for the terminal velocity as a function of diameter (Rogers and Yau, 1991, Chap. 8),

$$V_t = \begin{cases} 2.98 \cdot 10^7 \cdot D^2 & 0 < D \leq 1.30 \cdot 10^{-4} \\ 4.00 \cdot 10^3 \cdot D & 1.30 \cdot 10^{-4} < D \leq 1.26 \cdot 10^{-3} \\ 1.42 \cdot 10^2 \cdot D^{1/2} & 1.26 \cdot 10^{-3} < D \leq 4.0 \cdot 10^{-3} \end{cases} \quad (9)$$

with velocity in m s^{-1} and diameter in m.

The larger the drops, the higher the deformation during the fall. Therefore, the cross section and the drag coefficient are greater than that for one sphere of equivalent volume. The increase of drop mass is compensated by the greater drag force. Beard (1976) found that for drops of over 5 mm diameter, terminal velocity is independent of size. For drops with diameter greater than 4 mm, the Best (1950) equation may be adopted,

$$v_t = v_{max}[1 - \exp(-D/\eta)]^{\lambda} \quad (10)$$

This equation is valid over a varied range of conditions. Mualem and Assouline (1986) indicate that for $v_{max} = 9.5$ m s^{-1}; $\eta = 1.32$ mm and $\lambda = 1.15$, it fits Gunn and Kinzer data very well (see Rogers and Yau, 1991, Table 8.1) for drops up to 6 mm in diameter. Here, this expression has been chosen for drops over 4 mm in diameter.

If the distance covered by the drop in its fall is not too large, it may hit the ground with less than the terminal velocity. Following Park *et al.* (1983), the impact velocity, v_{im}:

$$v_{im} = [v_t^2 - (v_t^2 - v_o^2)\exp(-2gh/v_t^2)]^{1/2} \quad (11)$$

where v_0 is initial velocity.

When the horizontal component of the velocity of water drops is not negligible, as in the case of sprinkler irrigation, or on windy days, the friction force changes direction along the path of the drops. In this case, the movement is described by the equations (von Bernuth and Gilley, 1984),

$$-C_2 v^2 \cos\theta = m d^2x/dt^2 \quad (12)$$

$$mg - C_2 v^2 \sin\theta = m d^2y/dt^2 \quad (13)$$

where C_2 is the new friction coefficient, θ the angle of the water path with the horizontal, and x and y the horizontal and vertical coordinates, respectively, from the nozzle of the sprinkler. These equations are solved by numerical methods to get the characteristics of the impact on the ground.

The practical significance of this modification is not great. Following Seginer (1965), a simple comparison of the water drop velocity generated with the rainfall simulator, with an initial velocity of 28 ms^{-1}, for a $\theta = 0°$ with similar drops under a vertical free fall, is shown in Fig. 4. For the drop size range of the rainfall simulator, the velocity of the drop along the parabolic path coincides with that of the vertical free fall after 5 m of the vertical path. The smaller the drop, the shorter the distance for the velocity to coincide. Therefore, impact velocity can be computed from Eqns. (9), (10), and (11).

Kinetic energy of water drops

The kinetic energy of a single drop, e_{ci}, with mass m_i and

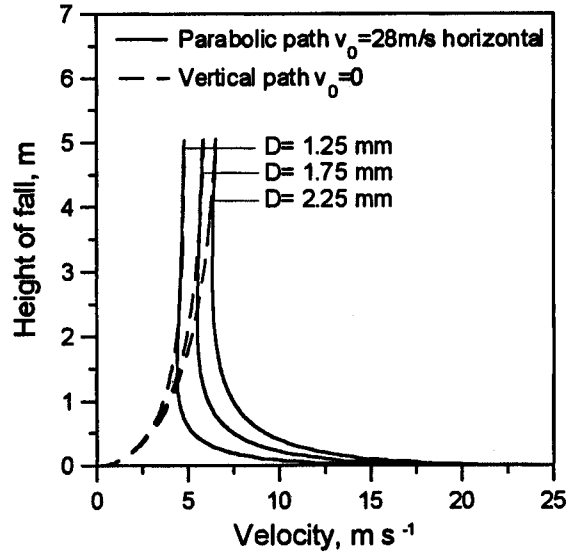

Fig. 4. *Velocities of water drops generated by the rainfall simulator, (continuous line), and freely falling, (discontinuous line), as a function of path length. Average raindrop height of fall from olive canopy is 2.5 m. Sprinkler height is 5 m.*

Table 2. Kinetic energy of simulated rainfall in the olive tree trial, and computed according to Brandt, (1990).

Ec J mm^{-1} m^{-2}			
Olive tree trial		Computed, (Brandt, 1990) h = 2.5m; r = 50 mm h^{-1}	
Rainfall simulator	15.7	Bare soil	23.3
Under canopy	17.1	Full surface cover	19.1
Modified by canopy	15.2		

impact velocity v_i, is given by:

$$e_{ci} = 1/2\ m_i v_i^2 \tag{14}$$

and that of the whole rainstorm, per unit of water volume, E_{co}

$$E_{co} = \sum_{i=1}^{n} \frac{N_i e_{ci}}{V_d} \tag{15}$$

where n is the number of size intervals, N_i the number of drops of the i interval, and V_d the total volume of drops.

The computed values are compared in Table 2. The kinetic energy under the canopy is greater than that of the rain falling outside. Water drops falling from the canopy, the gravity drops, belong to the high erosivity range of Moss (1989; Fig. 6). As Loch (1996) discussed, there may be little or no soil loss reduction under a canopy. In this case there is a net increase; this may lead to soil denudation if the litter under the tree disappears by agricultural management like harvesting fallen olive fruit, tillage and grazing. The fraction of kinetic energy due to canopy dripping is 0.89 multiplied by the whole kinetic energy under the canopy. Brandt (1990) stated that the kinetic energy of the rainfall under a full canopy cover, $E_c(1)$, depends not on rainfall rate, but on fall height (h) and on the distribution of the intercepted rain. She proposed, for a rain with D_{50} = 5 mm,

$$E_c(1) = 15.8h^{1/2} - 5.87 \tag{16}$$

where kinetic energy is written in J mm^{-1} m^{-2} and the height of fall in m. For any other fraction of surface cover, a linear interpolation between the above expression and the bare soil value, $E_c(0)$, may be made. Her expression for the latter case is:

$$E_c(0) = 8.95 + 8.44 \log r \tag{17}$$

with rainfall rate expressed in mm h^{-1}. The values of $E_c(1)$ and $E_c(0)$ for h = 2.5 m and r = 50 mm h^{-1} appear in Table 2. The kinetic energy estimated under the canopy is similar to that obtained by the Brandt expression. However, this equation overestimates the values obtained in the open in the present study. This result indicates that natural rain may be more erosive than the simulated rain.

Runoff generation

The presence of the tree canopy reduces the effective rainfall rate, increases the evaporation from branches, leaves, flowers and fruits, and diverts part of the water to stemflow. This stemflow, collected in different trials, resulted in a mean value of runoff which corresponds to 8% of the rain reaching the ground under the canopy. Due to the disposition of the sprinklers in the rainfall simulator, the rainfall rate was higher under the canopy than outside, irrespective of interception effects.

Some of the hydrographs recorded during the field trials are shown in Fig. 5, where the area under the canopy is separated from the rest of the plot. The rain starts at zero time. In general, runoff under the canopy starts and ends later, possibly due to the retarding effect of the interception process.

Canopy storage starts to fill up from a dry state and an important fraction of rainfall is retained. A similar effect was found by Loch and Donnollan (1988) caused by the plant residue left over the soil surface. Mohamoud and Ewing (1990) estimated a great reduction of the rainfall rate in the first minute of the rain event. The interception of the canopy may control soil erosion in events of small intensity or duration. After rainfall ceases, there is an additional contribution of runoff from the last water drops dripping from the canopy, as well as from the stem of the tree. These fluctuations in flow are due to small changes in the water pressure in the pumping system, and to wind speed changes which are reflected quickly in the runoff. The same trend is observed in the sediment concentration graphs.

Runoff hydrographs respond to the rain input in a form resembling that of the kinematic wave equation, (Laguna and Giráldez, 1993). A simple check on whether the use of the kinematic wave approach is apposite might be the estimation of equilibrium time, the time after which a constant rate of effective rainfall would yield a constant rate of runoff. According to the kinematic wave model, this equilibrium time, t_e, is expressed as

$$t_e = \left[\frac{L r_e^{(1-n)}}{\sigma}\right]^{1/n} \tag{18}$$

where L is the surface length; r_e the effective rainfall rate and σ the coefficient of the potential relationship between water depth and flow rate, used as the simplification of the momentum conservation equation in the Saint-Venant equations for the surface water flow, (e.g. Chow *et al.*, 1988; § 9.1) with n as the exponent. This coefficient is a measure of the surface roughness for water flow, the hydraulic roughness for Hairsine *et al.* (1992). Figure 6

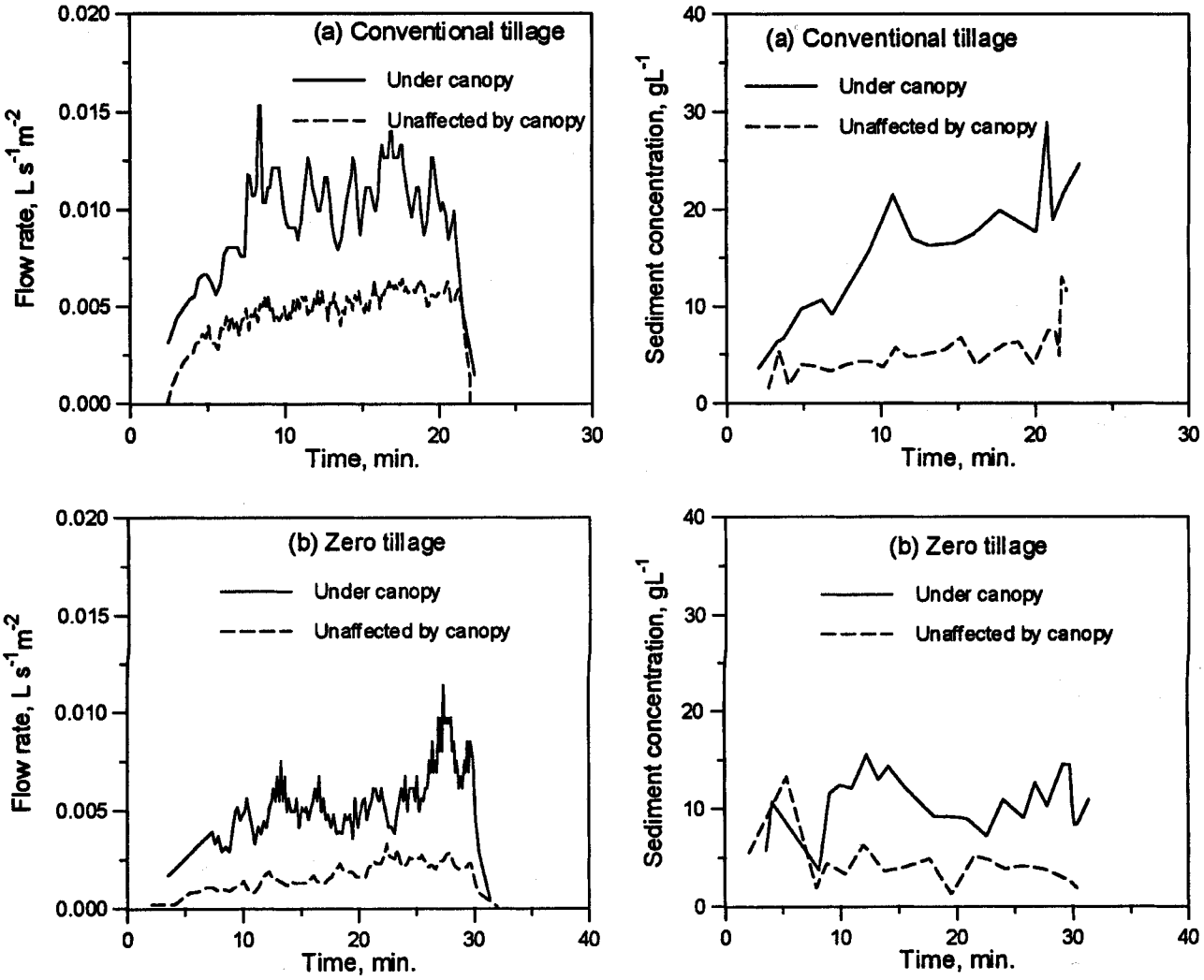

Fig. 5. *Hydrographs, and sediment concentration curves as a function of time for (a) the conventionally tilled and (b) non-tilled soil plots. The contributions of the areas under and outside the canopy are represented by different curves.*

shows the time to equilibrium and equilibrium flow rate for the different treatments. From Eqn. (18), a logarithmic transformation allows a linear relationship with an easy fit to experimental data. The fitted values of hydraulic roughness collected in Table 3, indicate that the values of the exponent are reasonably within the range given by authors such as Wooding (1965). Soil surface is apparently rougher in the tilled than in the untilled soil, as well as under the canopy than outside the canopy. The greater difference in the hydraulic behaviour of the surface is due to the tillage treatment.

In general, the water yield is greater in conventionally tilled soils than in zero-tilled soils, Fig. 7; this may be attributed to the formation of a shallow plough sole. Some compaction due to gravity drops may be responsible for a certain increase of the water yield under the canopy.

Sediment yield

The modification of gravity drops under the tree detaches more soil particles than natural raindrops. Consequently, soil losses are greater under the canopy than outside it, as may be appreciated in the graphs of Fig. 8. As the kinetic energy of raindrops increases, so does the mass of sediments in runoff at the outlets of the respective plots. This trend is not so clear in the tilled soils, possibly due to the lack of surface uniformity caused by the tillage implement. The tendency is clearer when kinetic energy is compared to sediment concentration under equilibrium conditions. The average values of soil lost per unit area and unit rain depth are given in Table 4.

Since the rainfall rates of the simulated events were too high, there were sufficient soil particles to make the erosion processes transport limited (Hairsine and Rose, 1992).

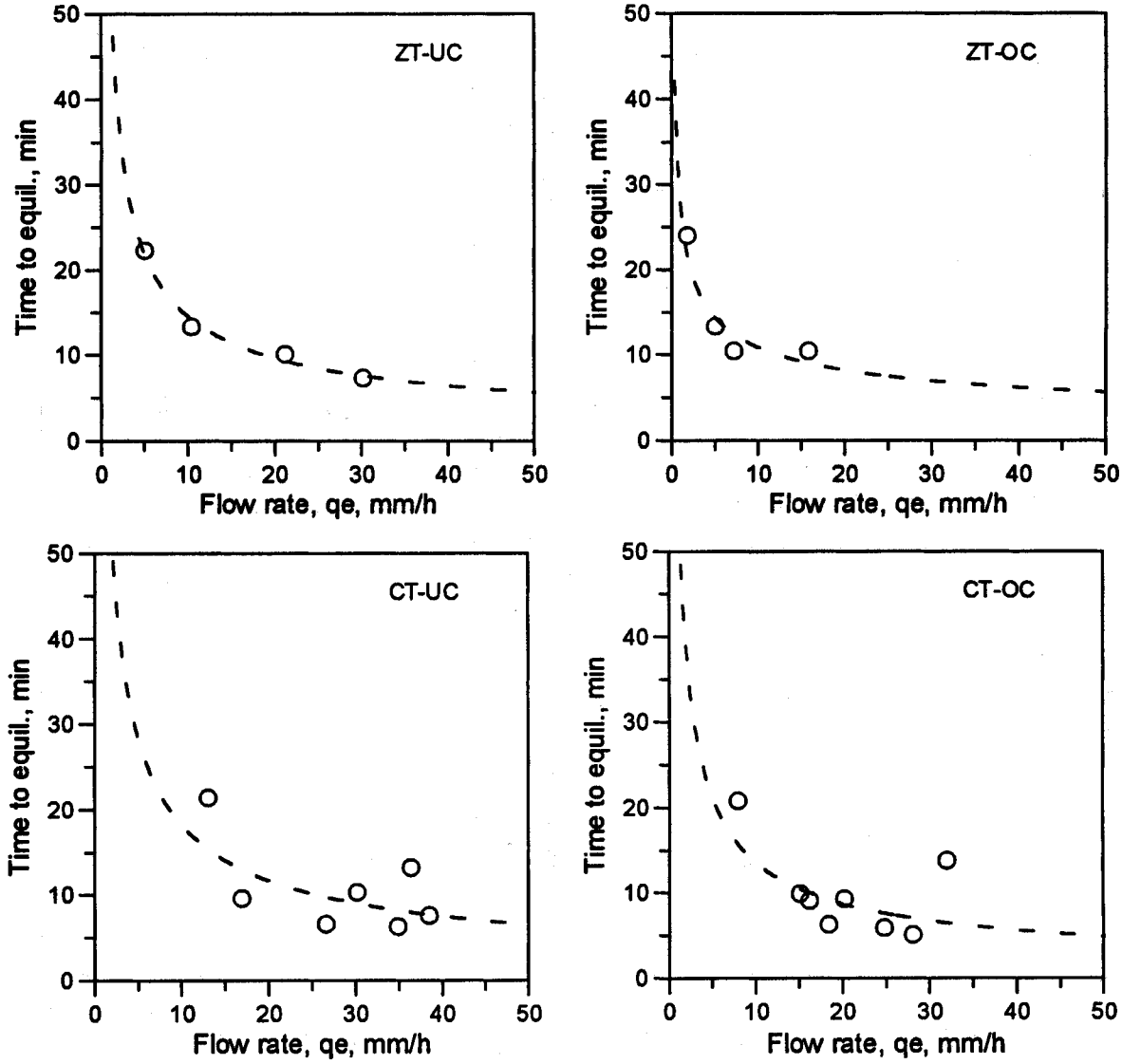

Fig. 6. *Relation between time at equilibrium and equilibrium flow rate for the experimental plots in the different experiments. In all cases the dashed line represents the kinematic wave equation. (ZT, zero tillage CT, conventional tillage UC, under canopy OC, outside canopy.)*

Therefore, the use of transport capacity expressions such as that used by Moore and Burch (1986a) in the soil erosion context may be tested. According to Yang (1973), the unit stream power, P, may be written as the product of flow velocity, v, and the slope of the soil surface, S, $P = vS$. Sediment transport capacity, c_t, is related to unit stream

Table 3. Parameters of the kinematic wave model for the surface water flow.

Treatment	Position with the canopy	Exponent n	Hydraulic roughness α	Correlation coefficient (log transf.)	Number of data pairs
Zero tillage	under	2.44	$2.66\ 10^{-4}$	0.9906	4
	outside	1.68	$1.89\ 10^{-2}$	0.9261	4
Conv. tillage	under	2.94	$1.08\ 10^{-5}$	0.6860	8
	outside	2.75	$6.93\ 10^{-5}$	0.5975	8

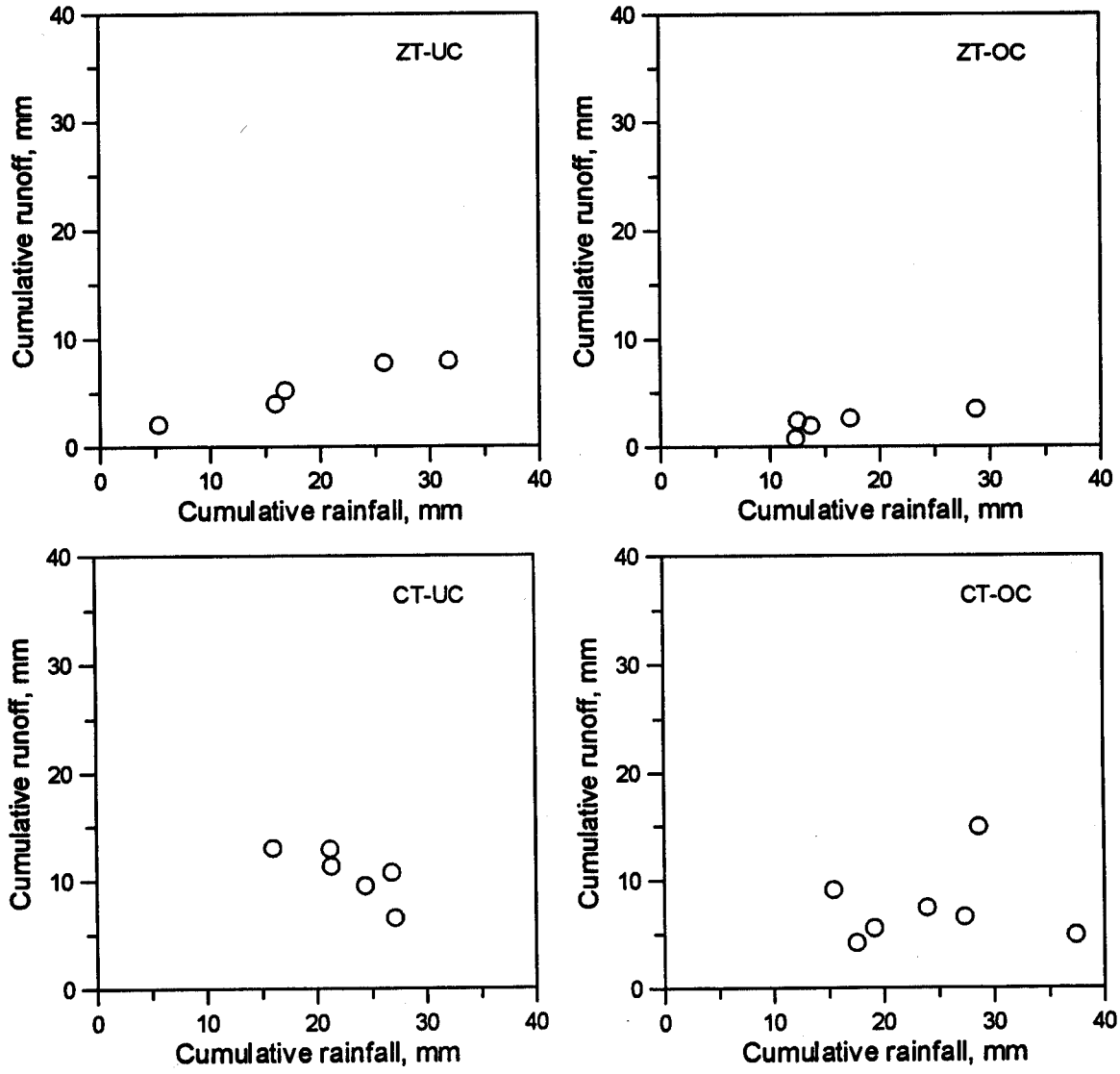

Fig. 7. *Comparison of the cumulative rainfall and runoff volumes for the conventionally (CT) and zero tilled (ZT) soils under (UC) and outside the canopy (OC) of the olive tree.*

power, after some simplifying assumptions (Moore and Burch, 1986b) by:

$$c_t = \delta P^{\varepsilon} = \delta \frac{q^{\frac{2\varepsilon}{5}} S^{\frac{13\varepsilon}{10}}}{n_M^{3/5}} = \zeta q^{\frac{2\varepsilon}{5}} \qquad (19)$$

after substitution of Manning uniform flow equation, with n_M as the roughness coefficient, q as the flow rate, and δ, ε, and ζ as parameters. If sediment is transported at the capacity rate, sediment concentration, c_s is approximated by c_t. Figure 9 shows that the fits of potential curves to the experimental data is good. The values found for the exponent ε (Table 5) differ little from unity as Moore and Burch (1986b) suggested. The Student's t statistics are included in the Table.

The size of sediment particles compared to the original soils, is shown in Table 6. The intensity of the erosion events mobilizes larger particles under the canopy than in the open space between trees. There is a larger proportion of large particles in the tilled soil than in the chemically weeded one.

Discussions and results

Tree canopy plays an important role intercepting radiant energy and rainfall, among other physiological functions. Nevertheless, it increases the risk of soil erosion in the surroundings of the trunk. Gravity drops are very common in many vegetable species, but their impact depends on the

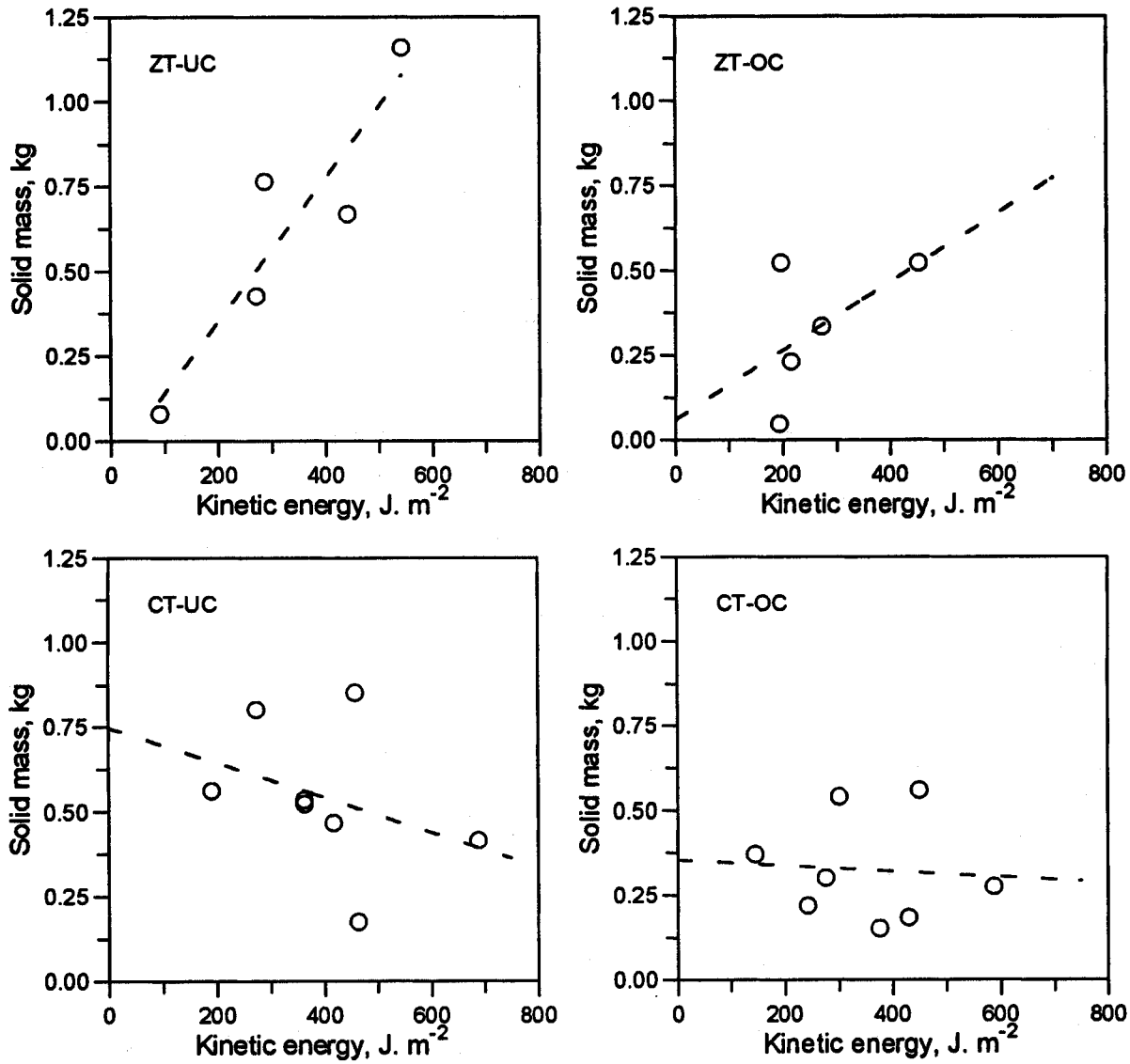

Fig. 8. *Relationship between kinetic energy and sediment concentration in runoff water for the experiments of Fig. 7.*

management system of the crop and the soil. In natural systems, the undergrowth, the mixture of decaying litter and small plants emerging between them, protects the soil.

Table 4. Average value of soil loss per unit area and per unit rain depth, g $mm^{-1}m^{-2}$, obtained in the different trials.

Treatment	Soil lost per unit area and rain depth g mm^{-1} m^{-2}	
	Under the canopy	Outside the canopy
Zero tillage	4.02	0.95
Conv. tillage	5.81	0.89

In cultivated areas, this layer may have disappeared by the time of the next rainfall. The magnitude of the soil loss under the canopy is therefore variable. In many olive cropped zones, olive trees remain as witnesses of the erosion processes, as Laguna and Giráldez (1990) have recorded. The soil surface relief in these areas results from the interaction of water and tillage, or mechanical erosion processes. Frequent passes of the disk harrow displace soil particles and leave a loose layer, which is easily removed by the next surface runoff event. The trees act as isolated barriers or piers producing a small mound upstream and a hollow downstream. Gravity drops contribute to this denudation.

The results presented here, although obtained in only a few field experiments, indicate the importance of the increase in kinetic energy of the raindrops, and its effect

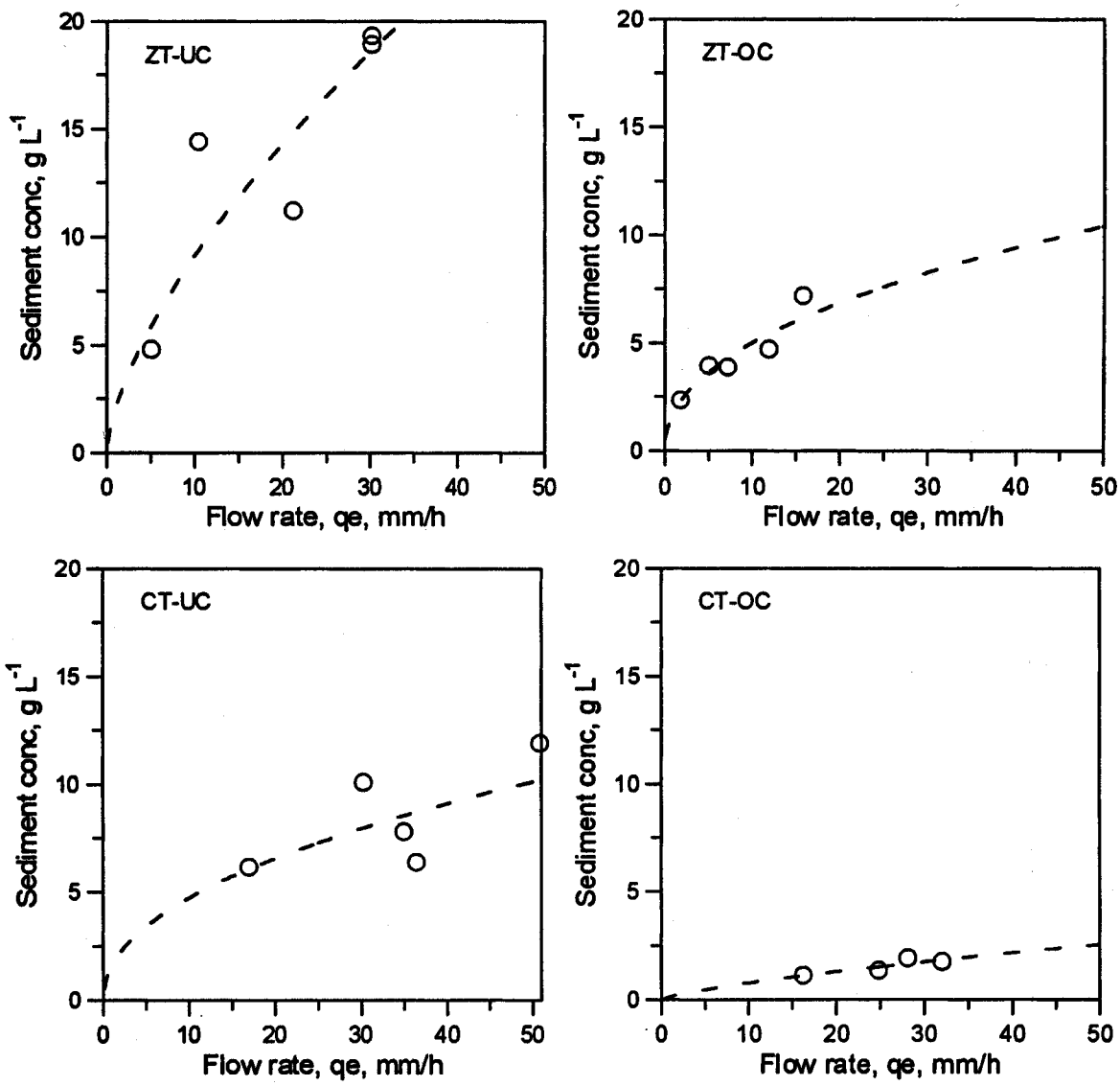

Fig. 9. *Relationship between sediment concentration and equilibrium flow rate in the experiments of Fig. 7.*

in soil detachment and transport. More research is needed to advise farmers and agronomists on a more rational management system. In the interception process, the role of canopy pruning, intensively practised in the southern olive growing region to obtain larger fruits, is another aspect that requires further attention.

Table 5. Parameters of the sediment concentration runoff flow rate relation, $c_s \approx \zeta q^{2\varepsilon/5}$.

Treatment	Position within the canopy	Coefficient ζ	Exponent $2\varepsilon/5$	Correlation coefficient (log transf.)	ε	Number of data pairs
Zero tillage	under	2.07	0.644	0.8752	1.61*	5
	outside	1.76	0.450	0.9530	1.13*	5
Conv. tillage	under	1.60	0.472	0.6632	1.18*	5
	outside	0.15	0.731	0.8944	1.75*	4

* Differences with unity not significant, Student's t statistics at the significance level $\alpha = 0.05$.

Table 6. Size distribution of aggregates in soil and runoff flow.

Particle size mm	Conventional tillage			Zero tillage		
		Sediment			Sediment	
	Soil	Under	Outside	Soil	Under	Outside
0.002-0.05	0.593	0.630	0.789	0.503	0.524	0.621
0.05-2.0	0.407	0.366	0.210	0.497	0.472	0.365

Conclusions

The olive tree canopy modifies the kinetic energy of raindrops, increasing their size to the point of overcoming the reduction in their terminal velocity, when compared to the free fall from above. While this reduction might not be significant in natural conditions because the litter layer of fallen leaves, fruit and broken twigs may dissipate a great part of the kinetic energy of the water drops, the common agricultural practice of tree foot sweeping prior to the harvest to pick up the fruits from the soil, leaves it unprotected.

The use of simple runoff and erosion models like the kinematic wave and transport capacity equations allows a characterization of the phenomena, indicating the differences between tilled and untilled soils, as well as the influence of the canopy on them.

Appreciable soil losses occur from conventionally tilled olive orchards, and it is recommended that conservation measures should be taken to preserve the natural environment in a rational way.

Acknowledgements

The authors acknowledge the collaboration of Juan de Haro, Bienvenido Dugo, Catalina Lara, Eli Ordoñez, Carmen del Moral and Araceli Nevado. The research was supported by the Plan Andaluz de Investigación of the Autonomous Government of Andalucia and by the Spanish Projects CICYT, OLI 96-2129 and INIA-CAO-98-011.

References

Assouline, S. and Mualem, Y., 1989. The similarity of regional rainfall: a dimensionless model of drop size distribution. *Trans. Amer Soc. Agric. Engs.*, **32**, 1216–1222.

Barfield, B.J. and Hirschi, M.C., 1986. Tipping bucket flow measurements on erosion plots. *Trans. Amer Soc. Agric. Engs.*, **29**, 1600–1604.

Beard, K.V., 1976. Terminal velocity and shape of cloud and precipitation drops aloft. *J.Atmos. Sci.*, **33**, 851–864.

Best, A.C., 1950. Empirical formulae for the terminal velocity of water drops falling through the atmosphere. *Quart. J. Roy. Meteorol. Soc.*, **76**, 302–312.

Brandt, C.J., 1989. The size distribution of throughfall drops under vegetation canopies. *Catena*, **16**, 507–524.

Brandt, C.J., 1990. Simulation of the size distribution and erosivity of raindrops and throughfall drops. *Earth. Surf. Process Land*, **15**, 687–698.

Chow, V.T., Maidment, D.R. and Mays, L.W., 1988. Applied Hydrology, McGraw-Hill, New York.

Eigel, J.D. and Moore, I.D., 1983. A simplified technique for measuring raindrop size and distribution. *Trans. Amer Soc. Agric. Engs.*, **26**, 1079–1084.

Gardner, W.H., 1986. Water content. In A. Klute, ed. Methods of Soil Analysis, Part 1. Physical and mineralogical methods, 2nd edition, Amer Soc. Agron. monog. 9, American Society of Agronomy, Madison, Cap. 21.

Gee, G.W. and Bauder, J.W., 1986. Particle-size analysis. In A. Klute, ed. Methods of Soil Analysis, Part 1. Physical and mineralogical methods, 2nd edition, Amer Soc. Agron. monog. 9, American Society of Agronomy, Madison, Cap. 15.

Giráldez, J.V., Carrasco, C., Otten, A., Iestwaart, H., Laguna, A. and Pastor, M., 1990. The control of soil erosion in olive orchards under reduced tillage. In A.G. Ferreira, M.A. Coutinho, and P.P. Tomas, eds. Interactions between agricultural systems and soil conservation in the Mediterranean Belt, Eur. Soc. Soil Conserv., Oeiras, Sep. 4–8.

Hairsine, P.B. and Rose, C.W., 1992. Modelling water erosion due to overland flow using physics principles: I Uniform flow. *Wat. Resour. Res.*, **28**, 237–243.

Hartley, D.M. and Alonso, C.V., 1991. Numerical study of the maximum boundary shear stress induced by raindrop impact. *Wat. Resour. Res.*, **27**, 1819–1826.

Laguna, A. and Giráldez, J.V., 1993. The description of soil erosion through a kinematic wave model. *J. Hydrol.*, **145**, 65–82.

Laguna, A. and Giráldez, J.V., 1990. Soil erosion under conventional management systems of olive tree culture. In A.G. Ferreira, M.A. Coutinho, and P.P. Tomas, eds. Interactions between agricultural systems and soil conservation in the Mediterranean Belt, Eur. Soc. Soil Conserv., Oeiras, Sep. 4–8.

Laws, J.O. and Parsons, D.A., 1943. Relation of raindrop size to intensity. *Trans. Amer Geophys. Un.*, **24**, 452–460.

Loch, R.J., 1996. Using rill/interrill comparisons to infer likely responses of erosion to slope length; implications for land management. *Aust. J. Soil Res.* **34**, 489–502.

Loch, R.J. and Donnollan, T.E., 1988. Effects of the amount of stubble mulch and overland flow on erosion of a cracking clay soil under simulated rain. *Aust. J. Soil Res.*, **26**, 661–672.

Mohamoud, Y.M. and Ewing, L.K., 1990. Rainfall interception by corn and soybean residue. *Trans. Amer Soc. Agric. Engs.*, **33**, 507–511.

Moore, I.D. and Burch, G.J., 1986a. Sediment transport capacity of sheet and rill flow: application of unit stream power theory. *Wat. Resour. Res.*, **22**, 1350–1360.

Moore, I.D. and Burch, G.J., 1986b. Physical bases of the length-slope factor in the Universal Soil Loss Equation. *Soil Sci. Soc. Amer J.*, **50**, 1294–1298.

Moss, A.J., 1989. Impact droplets and the protection of soils by plant covers. *Aust. J. Soil Res.*, **27**, 1–16.

Nearing, M.A., 1987. Theoretical one-dimensional water to soil impact pressures. *Trans. Amer Soc. Agric. Engs.*, **30**, 369–373.

Park, S.W., Mitchell, J.K. and Bubenzer, G.D., 1983. Rainfall

characteristics and their relation to splash erosion. *Trans. Amer Soc. Agric. Engs.*, **26**, 795–804.
Pastor, M., 1987. Sistemas de manejo de suelo en el olivar, unpubl. Ph.D. diss., Dept. of Agronomy, University of Córdoba.
Pruppacher, H.R. and Klett, J.D., 1980. Microphysics of clouds and precipitation. Reidel, Dordrecht.
Rogers, R.R. and Yau, M.K., 1991. A short course in cloud physics, 3ed. Pergamon Press, Oxford.
Rose, C.W., 1960. Soil detachment caused by rainfall. *Soil Sci.*, **89**, 28–35.
Salles, C., Poesen, J., and Borselli, L., 1999. Measurement of simulated drop size distribution with an optical spectro pluviometer: sample size considerations. *Earth Surf. Process. Land*, **24**, 545–556.
Seginer, I., 1965. Tangential velocity of sprinkler drops. *Trans. Amer Soc. Agric. Engs.*, **8**, 90–93.
Sempere-Torres, D., Salles, C., Creutin, J.-D. and Delrieu, G., 1992. Quantification of soil detachment by raindrop impact: performance of classical formulae of kinetic energy in Mediterranean storms. In J., Bogen, D.E. Walling, and T.J., Day, eds. Erosion and sediment transport monitoring programmes in river basins IASH Publ. no. 210, 115–124.
Sempere-Torres, D., Porra, J.M. and Creutin, J.D., 1994. A general formulation for raindrop size distribution. *J. Appl. Meteorol.*, **33**, 1494–1502.
Sharma, P.P., Gupta, S.C. and Foster, G.R., 1993. Predicting soil detachment by raindrops. *Soil Sci. Soc. Amer J.*, **57**, 674–680.
von Bernuth, R.D. and Gilley, J.R., 1984. Sprinkler droplet size distribution estimation from single leg test data, *Trans. Amer Soc. Agric. Engs.*, **27**, 1435–1441.
Wooding, R.A., 1965. A hydrologic model for the catchment-stream problem. I. Kinematic wave theory. *J. Hydrol.*, **3**, 254–267.
Yang, C.T., 1973. Incipient motion and sediment transport. *J. Hydraul. Div. A.S.C.E.*, **99**, 1679–1704.
Zhai, R., Kachanoski, R.G. and Voroney, R.P., 1990. Tillage effects on the spatial and temporal variations of soil water. *Soil Sci. Soc. Amer J.*, **54**, 186–192.